ELSEVIER

Journal of Organometallic Chemistry 561 (1998) 109–120

Journal of Organometallic Chemistry

Substituents effects on the addition of silyllithium and germyllithium to C_{60}

Takahiro Kusukawa, Wataru Ando *

Department of Chemistry, University of Tsukuba, Tsukuba, Ibaraki 305, Japan

Received 2 December 1997; received in revised form 3 February 1998

Abstract

Mono-adducts **2** and di-adducts **3** are obtained by the reaction with silyllithium and germyllithium **1** with C_{60}. The selectivities of the products are controlled by electronic and steric effects of the substituents. Formations of 1,4-adduct **4** and dimer **5** can be obtained in the presence of biphenyl derivatives. © 1998 Elsevier Science S.A. All rights reserved.

Keywords: Fullerene; Silylanion; Germylanion

---

1. Introduction

Recently, fascinating reactions have been discovered in the fuctionalization of fullerene by a carbon nucleophile. The reactions of lithium and Grignard reagents with C_{60} have been reported to produce mono-alkylated (RHC_{60}) or mono-arylated ($ArHC_{60}$) products [1–4], and few cases for bis-alkylated (R_2C_{60}) and bis-arylated (Ar_2C_{60}) products ([4]e,g). Despite numerous elegant efforts to the carbon nuclophilicity, far less attention has been devoted to mechanistic information for the bis-adduct. Recently we have shown that reaction of silyllithium end C_{60} gives three products, 1,2[6,6 addition]-, 1,4-adducts and 1,16-bis-silyl adduct (Scheme 1). Analyzing the data set of reaction for fullerene and silyllithium, the steric effect of silyllithium is not only essential for the product selectivity but also electronic effect is of importance for the product selectivity. In this study, a number of differently substituted silyllithium and germyllithium reagents have been prepared and the effects of substitution are compared for the product selectivity. The electronic effect is supported by semiempirical calculations [5].

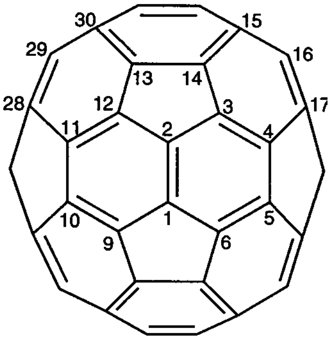

Chart 1

2. Results and discussions

2.1. Reactions of silyllithium and germyllithium reagents with C_{60}

A THF solution of silyllithium 1 (81.3 mmol) was slowly added to a vigorously stirred solution of C_{60} (81.3 mmol) in toluene at −78°C under an argon atmosphere to afford immediately a black suspension. After addition of EtOH gave a dark brown solution, followed by means of gel-permeation chromatography to produce pure adducts (Table 1). In the case of diisopropylphenylsilyllithium **1a** and isopropyldiphenylsilyllithium **1b**, mono-adduct **2** was obtained as a sole product. In the reactions of di-*tert*-

---

* Corresponding author. Tel.: +81 298 536503.

PII S0022-328X(98)00497-5

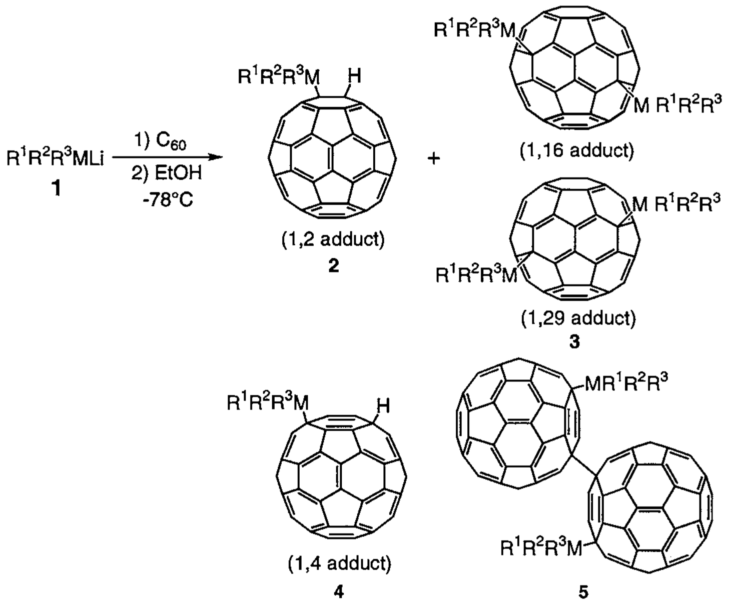

a: M = Si, $R^1 = R^2 =$ *iso*-Pr, R^3 = Ph
b: M = Si, R^1 = *iso*-Pr, $R^2 = R^3$ = Ph
c: M = Si, R^1 = *tert*-Bu, $R^2 = R^3$ = Ph
d: M = Si, $R^1 = R^2 = R^3 = Me_3Si$
e: M = Si, $R^1 = R^2$ = *tert*-Bu, R^3 = Ph
f: M = Si, $R^1 = R^2$ = *tert*-Bu, R^3 = 4-Me-C_6H_4-
g: M = Si, R^1 = *tert*-Bu, $R^2 = R^3$ = 4-Me-C_6H_4-
h: M = Ge, $R^1 = R^2$ = *iso*-Pr, R^3 = Ph
i: M = Ge, $R^1 = R^2$ = *tert*-Bu, R^3 = Ph

Scheme 1.

butylphenylsilyllithium **1d** and tris(trimethylsilyl)silyllithium **1e** (with C_{60}), bis-adduct **3** was obtained as a sole product. Additionally, 4-methylphenyl group substituted silyllithium reagents **1f** and **1g** gave adducts **2**, **3**, **4** and **5** (Scheme 1, Table 1, Chart 1). Similarly, diisopropylphenylgermyllithium **1h** reacts with C_{60} to give mono-adduct **2h** upon quenching with EtOH (Scheme 1, Table 1, Chart 1). Under similar conditions, di-*tert*-butylphenylgermyllithium **1i** reacts with C_{60} to give bis-adduct **3i** in high yield. However, attempted reactions of C_{60} with Ph_3SiLi were unsuccessful and formation of brown precipitate was observed at − 78°C, C_{60} was recovered upon quenching with EtOH. The analogous reaction with other silyllithium ($Me_2PhSiLi$, $MePh_2SiLi$, $Et_2PhSiLi$, $EtPh_2SiLi$) also leads to unsuccessful results.

2.2. Reaction in the presence of biphenyl

The formation of **4** and **5** poses a question on the mechanism of the addition of silyllithium to C_{60}. We carefully examined the reason for the formation of **4** and **5**. The reaction of *tert*-butyldiphenysilyllithium **1c** with C_{60} gave mono-adduct **2c** and bis-adduct **3c**. When we added *tert*-butyldiphenylsilyllithium **1c** to the toluene solution of C_{60} and 4,4′-dimethylbiphenyl at − 78°C, gave **3c** and **5c** was obtained after 30 min. in 53 and 28% yields, respectively (artTable 2). If we added *tert*-butyldiphenysilyllithium **1c** rapidly (5 min) to the solution of C_{60} and 4,4′-dimethylbiphenyl, **3c**, **4c** and **5c** was obtained in 34, 29 and 17% yields, respectively. Similar results were obtained in the presence of biphenyl (Table 2). We can not understand the effect of bipheny at present time, but the presence of biphenyl derivative promotes the formation of adducts **4** and **5**.

2.3. Spectroscopic structural characterization of *2*, *3*, *4*, and *5*

The FAB mass spectrum of **2a** exhibits at *m/z* 912–915 ($C_{60}(^{i}Pr_2PhSi)H$, $M^+ + 1$, molecular cluster ion). The ^{13}C-NMR spectrum of **2a** displays 30 signals for C_{60} carbons, supporting C_s symmetry for the molecule. One signal has a relative intensity of 4, one signal has a relative intensity of 3, 25 signals have a relative intensity of 2, and three signals have a relative intensity of 1; thus, the number of carbon atoms sums up to 60. Of the 30, two fullerene carbon atoms resonate at 58.87 and 60.94 ppm. The signals of all other carbons appear in the region between δ 130–160 ppm. The presence of one hydrogen connected to C_{60} is deduced from one doublet at 58.87 ppm and one singlet at 6.93 ppm in the ^{13}C- and ^{1}H-NMR spectrum, respectively. Regarding the addition pattern of the fullerene moiety, a 1,2[6,6]-addition is most probable. In the case of a 1,6-addition, observation of 60 signals of C_{60} carbons would be expected. The possibility of 1,4-addition can be eliminated by ^{13}C–^{1}H COLOC (Correlation Spectroscopy

Table 1
Reactions of silyllithium and germyllithium reagents with C_{60}

Lithium reagents	Product and yield (%)[a]			
	2	**3**	**4**	**5**
1a	78			
1b	80			
1c	50	22		
1d		69		
1e		72		
1f	11	42	11	6
1g		29	19	7
1h	76			
1i		87		

[a] Isolated yield.

via Long-range Coupling) spectroscopic method. It was shown that the proton resonance at 6.93 ppm correlates to the quaternary carbon (60.94 ppm, bonded to the silicon atom) on the C_{60}. The structure of the adduct **2b** was determined in a similar manner by use of NMR techniques. The FAB mass spectra of **3d** exhibit at *m*/*z* 1215–1218 ($C_{60}[(Me_3Si)_3Si]_2$, $M^+ + 1$, molecular cluster ion). The ^{13}C-NMR spectrum of **3d** displays 29 signals for all quaternary carbon. One signal has a relative intensity of 4, 28 signals have a relative intensity of 2, supporting C_2 symmetry for the molecule. Of the 29, one fullerene carbon atom resonates at 60.88 ppm.

Additions of two $(Me_3Si)_3Si$ groups are unfavorable to the 1,2[6,6 addition], 1,6[5,6 addition] and 1,4 positions by the steric hindrance, so the two $(Me_3Si)_3Si$ groups might be bonded to the 1,16 (1,29, 1,16 and 1,29 are enantiomer to each other) positions. The ^{13}C-NMR spectrum of **4f** displays 53 signals for all C_{60} carbons. Of the 53, one fullerene carbon atom resonates at 62.37 ppm. The presence of one hydrogen connected to C_{60} is deduced from one doublet at 49.54 ppm and one singlet at 5.44 ppm in the ^{13}C- and ^{1}H-NMR spectra, respectively. From these findings, 1,4-adduct is most probable for **4f**. The MALDI-TOF mass spectrum of **5f** exhibits at *m*/*z* 1907 ($[C_{60}(^tBu_2(4\text{-}MeC_6H_4)Si)]_2$, $M^+ + 1$). The ^{13}C-NMR spectrum of **5f** displays 57 signals for all quaternary carbons. Of the 57, two fullerene carbon atom resonates at 75.49 and 62.19 ppm. To clarify the structure of dimer **5**, we examined NMR experiment of **5c** with $^nBu_3SnH$ under thermolysis conditions [6]. When **5c** was allowed to react with $^nBu_3SnH$ (excess) in toluene-d^8 at 60–100°C for few minutes, **4c** was obtained as a major product (Fig. 1). From these findings, 1,4-dimer is most probable for **5f**. The UV–vis absorption spectrum of **2a** shows absorption at 417 and 445 nm. On the other hand, 1,16 and 1,29 adducts **3d** show characteristic broad absorption at 520–600 nm. Additionally UV–vis spectra of **4c** and **5c** show broad absorption at 440–450 nm which is characteristic to the 1,4-addition mode [7] (Fig. 2).

2.4. X-ray structural analysis of 3

In order to obtain information of the structure for **3d**, we carried out the X-ray crystallographic analysis. Modification **3d** crystallized in the triclinic space group $P\bar{1}$, with two enantiomers of **3d** and two CS_2 molecules in the unit cell, and the crystal structure of **3d** is shown in Fig. 3. Selected crystallographic data are listed in Table 3, interatomic distances and angles are listed in Tables 4 and 5. The C–C bond lengths C(2)–C(3), C(6)–C(5), C(4)–C(17), and C(14)–C(15) are within 1.368(6)–1.396(6) Å, which are close to the C–C double bond length.

2.5. Relative stability of C_{60}-adducts

The structure of **3d** is a new addition mode to the C_{60}. Relative stability of the dihydrofullerenes ($C_{60}H_2$) has been reported by Dixon with semiempirical calculations (Chart 2); 1,2[6,6 addition] (776.1 kcal mol^{-1}) $>$ 1,4 (780.0 kcal mol^{-1}) $>$ 1,16 or 1,29 (791.6 kcal mol^{-1}) $>$ 1,6[5,6 addition] (794.5 kcal mol^{-1}) [8]. 1,16 or 1,29 addition mode is 15.5 kcal mol^{-1} less stable than 1,2[6,6 addition] form, but 2.9 kcal mol^{-1} more

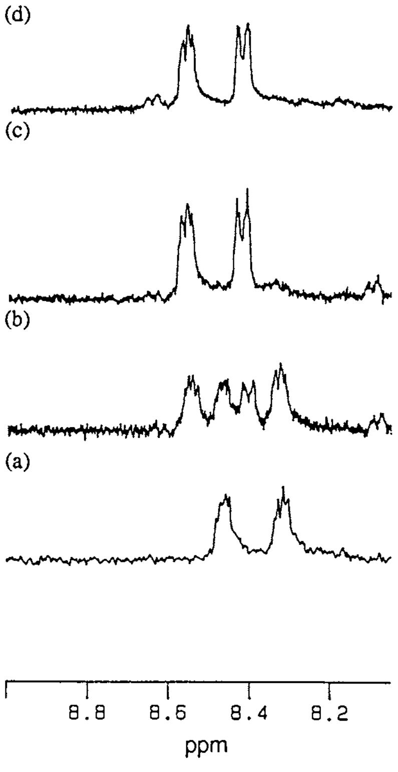

Fig. 1. Thermal reaction of **5c** with $^nBu_3SnH$ which shows only two pair of doublet at *ortho*-position. (a), **5c** with $^nBu_3SnH$ at r.t.; (b), **5c** with $^nBu_3SnH$ at 60°C for 5 min; (c), **5c** with $^nBu_3SnH$ at 100°C for 5 min; (d), authentic sample of **4c**.

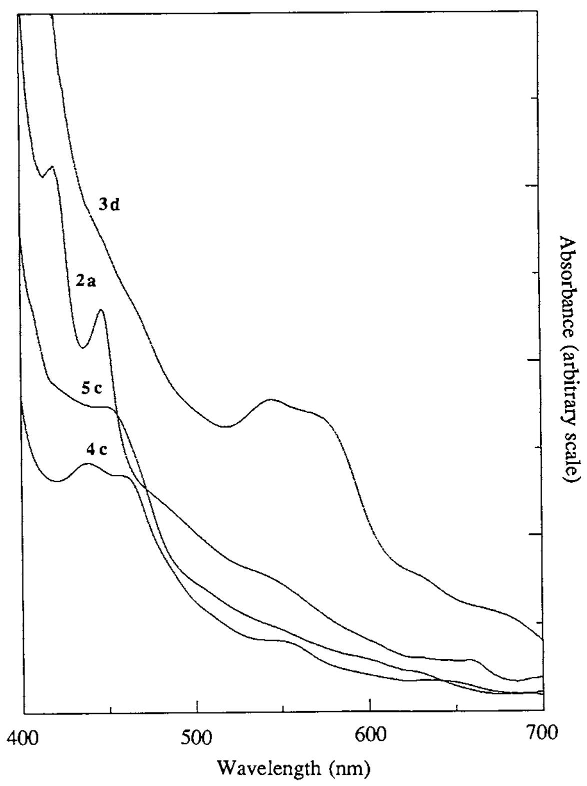

Fig. 2. UV–vis spectrum for **2**, **3**, **4** and **5** in toluene.

stable than 1,6[5,6 addition] form. To clarify the reason for the formation **3**, we calculated the stability of **3d** by means of AM1 method: 1,6[5,6 addition] (1041.6 kcal mol^{-1}) $>$ 1,2[6,6 addition] (1024.8 kcal mol^{-1}) $>$ 1,4 (987.5 kcal mol^{-1}) $>$ 1,16 or 1,29 (977.9 kcal mol^{-1}). Results of these calculations suggest that the formation 1,6-adducts might be controlled with steric effects of substituents.

The difference of the reactivity of silyllithium reagents presents a question on the mechanism. Additionally, we examined the semiempirical calculations of hydrosilanes instead of silyllithium reagents [9]. Electron-releasing substituents favors the formation of **2** and **3**. In the case of less electron- releasing substituents (Ph_3SiH, Me_2PhSiH, $MePh_2SiH$ etc.), we could not obtained corresponding C_{60} adducts (vice supra). From these findings, one possible mechanism for the formation of adducts **2** and **3** should involve the electron transfer from silyllithium to C_{60} (Scheme 2).

3. Experimental details

3.1. General

^1H-, ^{13}C- and ^{29}Si-NMR spectra were recorded on Bruker AM500 (500 and 125 MHz), AC400 (400, 100 and 80 MHz) and AC300 (300, 76 and 60 MHz) instruments. Mass spectra were obtained on Shimadzu QP-5000 and JEOL JMS SX 102A mass spectrometers. Elemental analyses were carried out by the Chemical Analytical Center of the University of Tsukuba. Gel permeation chromatography (GPC) was performed on a LC 908 instrument (Japan Analytical Industry) with a series of Jaigel 1H and 2H columns and toluene as eluent. The AM1 and PM3 calculations were conducted using standard methods as implemented in the MOPAC 6.0 semiempirical molecular orbital package on a Silicon Graphics IDIGO2 machine. All solvents, and reagents were purified according to standard procedures.

3.2. Materials

Diisopropylphenylsilyllithium(**1a**) [10], *tert*-butyldiphenylsilyllithium (**1c**) [11] and diisopropylphenylgermyllithium (**1h**) [10], tris(trimethylsilyl)silyllithium were prepared by the published procedure.

3.3. Preparation of bis(4-methylphenyl)-*tert*-butylsilane

3.3.1. General procedure, method A

A solution of *tert*-butyllithium (52 ml, 81.3 mmol) in pentane was added to a cooled (− 30°C) solution of 20.0 g of bis(4-methylphenyl)chlorosilane (81.3 mmol) in 40 ml of hexane. The mixture was warmed to r.t. for 6 h. All solids were removed by filtration, the solvent was evaporated, and the residue was fractionally distilled under reduced pressure to give 18.7 g (86%) of bis(4-methylphenyl)-*tert*-butylsilane as a colorless liquid, b.p. 119–121°C/3 Torr. ^1H-NMR (300 MHz, $CDCl_3$) δ 1.64 (s, 9H), 2.81 (s, 6H), 5.26 (s, 1H), 7.67 (d, 4H, $J = 7.7$ Hz), 8.13 (d, 4H, $J = 7.7$ Hz); ^{13}C-NMR (75.5 MHz, $CDCl_3$) δ 17.8 (s), 21.4 (q), 27.6 (q), 128.7 (d), 130.4 (s), 135.7 (d), 139.0 (s); MS *m/e* 268 (M^+); HRMS Calcd for$C_{15}H_{24}Si$: 268.1647. Found: 268.1652.

Di-*tert*-butyl(4-methylphenyl)silane was prepared from 20.0 g of dichloro(4methylphenyl)silane (105 mmol) according to method A, giving 19.3 g (79%) of colorless liquid, b.p. 88–90°C/3 Torr. ^1H-NMR (300 MHz, $CDCl_3$) δ 1.10 (s, 18H), 2.40 (s, 3H), 3.91 (s, 1H), 7.21 (d, 2H, $J = 7.6$ Hz), 7.52 (d, 2H, $J = 7.6$ Hz); ^{13}C-NMR (76 MHz, $CDCl_3$) δ 19.0 (s), 21.5 (q), 29.0 (q), 128.35 (d), 131.7 (s), 135.8 (d), 138.6 (s); MS *m/e* 234 (M^+); HRMS Calcd for $C_{15}H_{26}Si$: 234.1804. Found: 234.1812.

Di-*tert*-butylphenylsilane was prepared from 20.0 g of dichlorophenylsilane (114 mmol) according to method A, giving 18.9 g (76%) of colorless liquid, b.p. 70–72°C/3 Torr. ^1H-NMR (300 MHz, $CDCl_3$) δ 1.03 (s, 18H), 3.84 (s, 1H), 7.2–7.4 (m, 3H), 7.5–7.6 (m, 2H); ^{13}C-NMR (76 MHz, $CDCl_3$) δ 19.0 (s), 28.9 (q), 127.5 (d), 128.9 (d), 135.5 (s), 135.8 (d); MS *m/e* 220 (M^+).

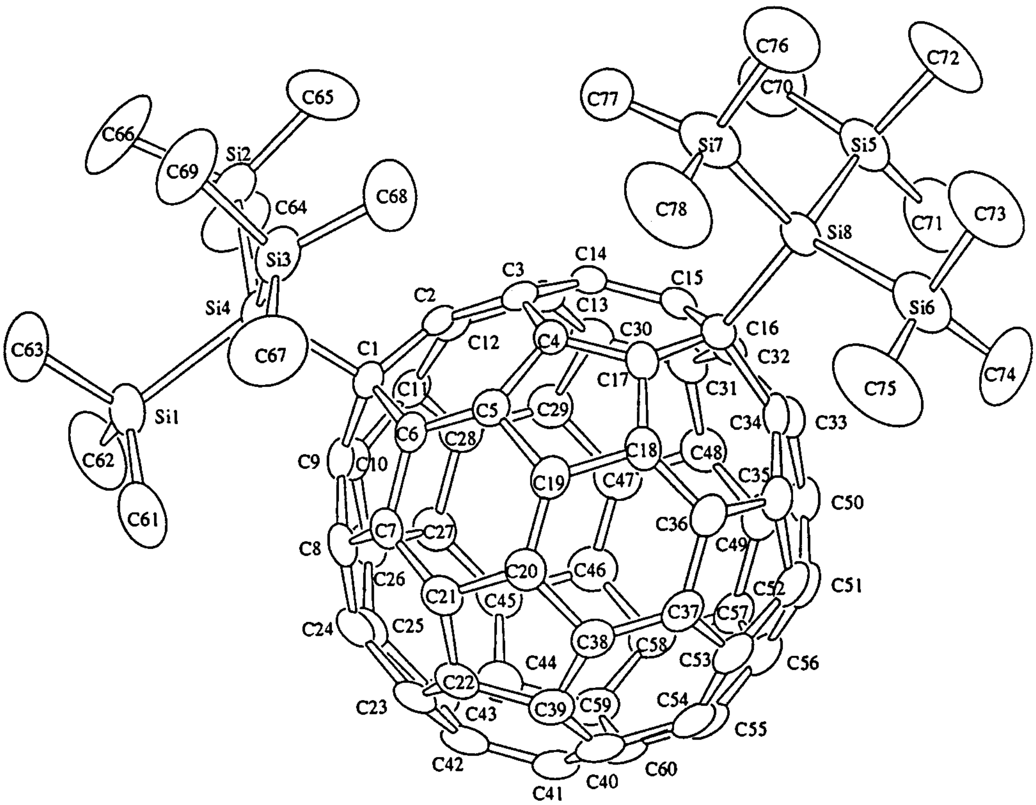

Fig. 3. Molecular structure of **3d**. Vibrational ellipsoids are shown at the 50% probability level. Two enantiomorphic molecules are present in the unit cell and one of them is shown.

3.4. Preparation of bis(4-methylphenyl)-tert-butylchlorosilane

3.4.1. General procedure, method B

A solution of 19.3 g of di-*tert*-butyl(4-methylphenyl)silane (82.5 mmol) and catalytic amount of benzoyl peroxide in 100 ml of CCl_4 was refluxed for 24 h. After evaporation of the solvent, the residue was fractionally distilled under reduced pressure to give 18.9 g (86%) of di-*tert*-butylchloro(4-methylphenyl)silane as a colorless liquid, b.p. 120–122°C/3 Torr. ^{1}H-NMR (300 MHz, $CDCl_3$) δ 1.16 (s, 18H), 2.42 (s, 3H), 7.25 (d, 2H, $J = 7.6$ Hz), 7.70 (d, 2H, $J = 7.6$ Hz); ^{13}C-NMR (76 MHz, $CDCl_3$) δ 21.4 (q), 22.1 (s), 28.1 (q), 128.42 (d), 129.2 (s), 134.9 (d), 139.5 (s); MS *m*/*e* 302 (M^+); HRMS Calcd for $C_{15}H_{23}ClSi$: 302.1258. Found: 302.1242.

Bis(4-methylphenyl)chloro-*tert*-butylsilane was prepared from 20.0 g of bis(4methylphenyl)-*tert*-butylsilane (74.6 mmol) according to method B, giving 19.9 g (88%) of colorless liquid, b.p. 143–145°C/3 Torr. ^{1}H-NMR (500 MHz, $CDCl_3$) δ 1.24 (s, 9H), 2.45 (s, 6H), 7.30 (d, 4H, $J = 7.7$ Hz), 7.75 (d, 4H, $J = 7.7$ Hz); ^{13}C-NMR 126 MHz, $CDCl_3$) δ 20.7 (s), 21.5 (q), 26.5(q), 128.7 (d), 129.1 (s), 135.2(d), 140.2(s); MS *m*/*e* 268 (M^+); HRMS Calcd for$C_{15}H_{25}ClSi$: 268.1414. Found: 268.1402.

Di-*tert*-butylchlorophenylsilane was prepared from 18.9 g of di-*tert*-butylphenylsilane (85.9 mmol) according to method B, giving 18.3 g (84%) of colorless liquid, b.p. 85–86°C/3 Torr. ^{1}H-NMR (300 MHz, $CDCl_3$) δ 1.21 (s, 18H), 7.3–7.5 (m, 3H), 7.7–7.9 (m, 2H); ^{13}C-NMR (76 MHz, $CDCl_3$) δ 22.1 (s), 28.1 (q), 127.6 (d), 129.6 (d), 132.8 (s), 134.9 (d); MS *m*/*e* 254 (M^+); HRMS Calcd for$C_{14}H_{23}ClSi$: 254.1258. Found: 254.1262.

3.5. Preparation of di-tert-butylchlorophenylgermane

A solution of phenyllithium (38 ml, 46.2 mmol) in Et_2O was added to a cooled (78°C) solution of 11.8 g of dichloro-di-*tert*-butylgermane (46.2 mmol) in 40 ml of hexane. The mixture was warmed to r.t. for 6 h. All solids were removed by filtration, the solvent was evaporated, and the residue was fractionally distilled under reduced pressure to give 11.1 g (80%) of di-*tert*-butylchlorophenylgermane as a colorless liquid, b.p. 90–91°C/1 Torr. ^{1}H-NMR (300 MHz, $CDCl_3$) δ 1.29 (s, 18H), 7.3–7.5 (m, 3H), 7.6–7.8 (m, 2H); ^{13}C-NMR (75 MHz, $CDCl_3$) 628.3 (q), 30.9 (s), 128.0 (d), 129.2 (d), 134.0 (d), 135.6 (s); MS *m*/*e* 300 (M^+).

Table 2
Reactions of *tert*-butyldiphenylsilyllithium (**1c**) with C_{60} in the presence of biphenyl derivatives[a]

Run	Time (min)	Additive	Yield (%)[b]			
			2c	**3c**	**4c**	**5c**
1	30	4,4′-Dimethylbiphenyl		53		28
2	30	Biphenyl	22	27		33
3	5	4,4′-Dimethylbiphenyl		34	29	17

[a] Condition, **1c** (139 μmol); C_{60} (139 μmol); additive (278 μmol); toluene (120 ml), −78°C.

[b] Isolated yield.

3.6. Preparation of isopropyldiphenylsilyllithium (*1b*)

3.6.1. General procedure, method C

Isopropyldiphenylchlorosilane [12] (1.00 g, 3.85 mmol) was stirred with excess lithium (100 mg, 14.4 mmol) in THF (7.5 ml) at r.t. for 24 h. The concentration of the solution was determined by titration against standardized *sec*-butyl alcohol *o*-phenanthroline as indicator. Di-*tert*-butylphenylsilyllithium (**1e**), di-*tert*-butyl(4-methylphenyl)silyllithium (**1f**), bis(4-methylphenyl)-*tert*-butylsilyllithium (**1g**), di-*tert*-butylphenylgermyllithium (**1i**) were also synthesized by general method C.

Table 3
Crystallographic data for **3d**

Empirical formula	$C_{79}H_{54}Si_8S_2$
Fw	1292.13
Crystal color, habit	red, needles
Crystal dimensions (mm)	0.10 × 0.20 × 0.40
Crystal system	Triclinic
Space group	$P\bar{1}$ (No. 2)
Unit cell dimensions	
a (Å)	9.921(2)
b (Å)	15.198(2)
c (Å)	21.523(2)
α (°)	82.79(1)
β (°)	85.36(1)
γ (°)	80.80(1)
V (Å^3)	3171.9
Z	2
D_{calc}	1.353
Radiation	Cu–K_α (λ = 1.54184 Å)
Temperature (°C)	23
Diffractometer	Enraf–Nonius CAD4
Scan type	$\omega-2\theta$
Rate (° min^{-1} in ω)	1–5
Scan width (°)	$(0.5+0.15\tan\theta)$
$2\theta_{max}$	119.9
Total reflections	9634
Unique reflections	9350
Struct soln., refinement	direct methods, full-matrix least squares
No. of observes ($I>3.00\sigma(I)$)	6934
No. of variables	802
R; *Rw*	0.065; 0.067

3.7. Reactions of silyllithium and germyllithium reagents with C_{60}

3.7.1. General procedure, method D

To a solution 100 mg of C_{60} (138.9 μmol) in 120 ml of dry toluene was added silyllithium and germyllithium (**1a–i**, 138.9 μmol) in THF over 30 min by syringe at −78°C. After the addition, the solution was quenched with EtOH, and anneal to the r.t.. The solvent was evaporated and the residue was purified by gel-permeation chromatography (Jaigel 1H and 2H columns, Japan Analytical Industry; eluent toluene, all of these products are unstable toward SiO_2), to afforded the adducts **2**, **3**, **4** and **5**.

2a: brown solid; ^{1}H-NMR (500 MHz, 1:2 $CDCl_3$-CS_2) δ 1.58 (d, 6H, $J = 7.5$ Hz), 1.73 (d, 6H, $J = 7.5$ Hz), 2.33 (sept, 6H, $J = 7.5$ Hz), 6.93 (s, 1H), 7.5–7.6 (m, 3H), 8.1–8.2 (m, 2H); ^{13}C-NMR (126 MHz, 1:2 $CDCl_3$–CS_2) δ 12.79 (d), 19.53 (q), 19.99 (q), 58.87 (d, 1C), 60.94 (s, 1C), 128.20 (d), 130.22 (d), 131.22 (s), 134.01 (s, 2C), 135.69 (s, 2C), 136.08 (d), 140.03 (s, 2C), 140.11 (s,2C), 141.19(s,2C), 141.28(s,2C), 141.41 (s, 2C), 141.58 (s, 2C), 141.69 (s, 2C), 142.10 (s, 2C), 142.33 (s, 2C), 142.38 (s, 2C), 143.35 (s, 2C), 144.29 (s, 2C), 144.40 (s, 2C), 144.52 (s, 2C), 145.18 (s, 2C), 145.32 (s, 2C), 145.35 (s, 2C), 145.95 (s, 3C), 146.10 (s, 2C), 146.18 (s, 2C), 146.21 (s, 2C), 146.48 (s, 1C), 147.08 (s, 4C), 147.42 (s, 2C), 153.87 (s, 2C), 157.36 (s, 2C); ^{29}Si-NMR (60 MHz, 1:2 $CDCl_3$–CS_2) δ 5.42; FAB-MS 912–915 ($M^+ + 1$ cluster); UV–vis (toluene) λ_{max} (nm): 417, 445.

2b: brown solid; ^{1}H-NMR (500 MHz, 1:2 $CDCl_3$–CS_2) δ 1.43 (d, 6H, $J = 7.3$ Hz), 2.35 (sept, 1H, $J = 7.3$ Hz), 7.03 (s, 1H), 7.5–7.6 (m, 6H), 8.2–8.3 (m, 4H); ^{13}C-NMR (126 MHz, 1:1 $CDCl_3$–CS_2) δ 11.88 (d), 19.19 (q), 59.29 (d, 1C), 60.68 (s, 1C), 128.33 (d), 130.39 (s, 2C), 130.62 (d), 134.53 (s, 2C), 135.70 (s, 2C), 136.98 (d), 140.10 (s, 2C), 140.22 (s, 2C), 141.38 (s, 4C), 141.52 (s, 2C), 141.69 (s, 2C), 141.81 (s, 2C), 142.20 (s, 2C), 142.44 (s, 2C), 142.47 (s, 2C), 143.40 (s, 2C), 144.47 (s, 2C), 144.53 (s, 2C), 144.61 (s, 2C), 145.31 (s, 2C), 145.37 (s, 2C), 145.46 (s, 2C), 146.02 (s, 2C), 146.08 (s, 2C), 146.21 (s, 2C), 146.30 (s, 2C), 146.32 (s, 2C), 146.63 (s, 1C), 147.20 (s, 1C), 147.32 (s, 2C), 147.47 (s, 2C), 153.95 (s, 2C), 157.03 (s, 2C); ^{29}Si-NMR(60 MHz, 1:1 $CDCl_3$–CS_2) δ 0.88; FAB MS 946–949 ($M^+ + 1$ cluster); UV–vis (toluene) iλ_{max} (nm): 417, 444.

2c: brown solid; ^{1}H-NMR (500 MHz, 1:2 $CDCl_3$–CS_2) δ 1.59 (s, 9H), 7.14 (s, 1H), 7.57.6 (m, 6H), 8.3–8.4 (m, 4H); ^{13}C-NMR (126 MHz, 1:1 $CDCl_3$–CS_2) 522.03 (s), 29.60 (q), 60.11 (d, 1C),60.99(s, 1C), 128.03(d), 130.35(d), 131.30 (s, 2C), 134.81 (s, 2C),

Table 4
Selected bond distances (Å)

Si(1)–Si(2)	2.369(2)	C(7)–C(21)	1.406(6)	C(32)–C(33)	1.471(7)
Si(1)–Si(3)	2.380(2)	C(8)–C(9)	1.449(7)	C(33)–C(34)	1.452(8)
Si(1)–Si(4)	2.366(2)	C(8)–C(24)	1.385(7)	C(33)–C(46)	1.376(7)
Si(1)–C(29)	1.990(5)	C(9)–C(10)	1.363(7)	C(34)–C(35)	1.385(8)
Si(2)–C(61)	1.868(8)	C(10)–C(11)	1.486(7)	C(35)–C(36)	1.452(9)
Si(2)–C(62)	1.856(9)	C(10)–C(26)	1;440(6)	C(35)–C(48)	1.452(7)
Si(2)–C(63)	1.878(8)	C(11)–C(12)	1.427(6)	C(36)–C(37)	1.455(8)
Si(3)–C(64)	1.853(7)	C(11)–C(28)	1.386(7)	C(37)–C(38)	1.388(8)
Si(3)–C(65)	1.864(7)	C(12)–C(13)	1.462(7)	C(37)–C(49)	1.450(8)
Si(3)–C(66)	1.864(8)	C(13)–C(14)	1.427(6)	C(38)–C(50)	1.432(7)
Si(4)–C(67)	1.870(8)	C(13)–C(30)	1.384(7)	C(39)–C(40)	1.393(8)
Si(4)–C(68)	1.860(9)	C(14)–C(15)	1.396(7)	C(39)–C(51)	1.443(7)
Si(4)–C(69)	1.857(8)	C(15)–C(16)	1.442(7)	C(40)–C(41)	1.445(7)
Si(5)–Si(6)	2.374(2)	C(15)–C(32)	1.455(8)	C(40)–C(52)	1.452(7)
Si(5)–Si(7)	2.361(3)	C(16)–C(17)	1.396(8)	C(41)–C(42)	1.473(7)
Si(5)–Si(8)	2.359(3)	C(16)–C(34)	1.452(8)	C(42)–C(43)	1.378(7)
Si(5)–C(1)	1.994(5)	C(17)–C(18)	1.461(7)	C(42)–C(53)	1.446(6)
Si(6)–C(70)	1.881(9)	C(18)–C(19)	1.452(8)	C(43)–C(44)	1.428(6)
Si(6)–C(71)	1.874(8)	C(18)–C(36)	1.392(8)	C(44)–C(45)	1.401(6)
Si(6)–C(72)	1.859(9)	C(19)–C(20)	1.388(8)	C(45)–C(46)	1.439(7)
Si(7)–C(73)	1.85(1)	C(20)–C(21)	1.435(7)	C(45)–C(54)	1.435(7)
Si(7)–C(74)	1.89(1)	C(20)–C(38)	1.459(8)	C(46)–C(47)	1.465(7)
Si(7)–C(75)	1.881(8)	C(21)–C(22)	1.453(7)	C(47)–C(48)	1.377(8)
Si(8)–C(76)	1.873(8)	C(22)–C(23)	1.372(7)	C(47)–C(55)	1.445(7)
Si(8)–C(77)	1.883(8)	C(22)–C(50)	1.458(7)	C(48)–C(49)	1.464(9)
Si(8)–C(78)	1.86(1)	C(23)–C(24)	1.464(7)	C(49)–C(57)	1.385(7)
C(1)–C(2)	1.502(8)	C(23)–C(51)	1.466(8)	C(50)–C(58)	1.395(8)
C(1)–C(6)	1.534(6)	C(24)–C(25)	1.442(8)	C(51)–C(59)	1.394(7)
C(1)–C(9)	1.521(6)	C(25)–C(26)	1.387(7)	C(52)–C(53)	1.449(8)
C(2)–C(3)	1.446(6)	C(25)–C(39)	1.456(7)	C(52)–C(60)	1.395(7)
C(2)–C(12)	1.390(7)	C(26)–C(27)	1.447(8)	C(53)–C(54)	1.379(7)
C(3)–C(4)	1.377(7)	C(27)–C(28)	1.462(7)	C(54)–C(55)	1.449(7)
C(3)–C(14)	1.446(7)	C(27)–C(41)	1.389(7)	C(55)–C(56)	1.399(8)
C(4)–C(5)	1.474(8)	C(28)–C(29)	1.509(7)	C(56)–C(57)	1.439(8)
C(4)–C(17)	1.443(7)	C(29)–C(30)	1.504(6)	C(56)–C(60)	1.442(7)
C(5)–C(6)	1.371(7)	C(29)–C(43)	1.539(6)	C(57)–C(58)	1.434(8)
C(5)–C(19)	1.448(7)	C(30)–C(31)	1.444(6)	C(58)–C(59)	1.431(7)
C(6)–C(7)	1.422(7)	C(31)–C(32)	1.377(6)	C(59)–C(60)	1.443(8)
C(7)–C(8)	1.439(6)	C(31)–C(44)	1.447(7)		

135.76 (s, 2C), 137.69 (d), 139.79 (s, 2C), 140.10 (s, 2C), 141.25 (s, 2C), 141.30 (s, 2C), 141.47 (s, 2C), 141.73 (s, 2C), 141.79 (s, 2C), 142.16 (s, 2C), 142.44 (s, 2C), 142.47 (s, 2C), 143.38 (s, 2C), 144.49 (s, 2C), 144.55 (s, 2C), 144.56 (s, 2C), 145.27 (s, 2C), 145.29 (s, 2C), 145.41 (s, 2C), 146.04 (s, 2C), 146.08 (s, 2C), 146.29 (s, 4C), 146.61 (s, 1C), 147.10(s, 1C), 147.39 (s, 2C), 147.60(s, 2C), 153.95 (s, 2C), 156.96 (s, 2C); ^{29}Si-NMR (60 MHz, 1:1 $CDCl_3$–CS_2) δ −0.46; FAB MS 960–963 ($M^+ + 1$ cluster); UV–vis (toluene) λ_{max} (nm): 417, 445.

3c: ^{1}H-NMR (500 MHz, 1:1 $CDCl_3$–CS_2) δ 1.45 (s, 9H), 7.3–7.5 (m, 6H), 7.93 (d, 2H, $J = 6.8$ Hz), 8.01 (d, 2H, $J = 6.8$ Hz); ^{13}C-NMR (126 MHz, 1:1 $CDCl_3$–CS_2) 522.32 (s), 29.16 (q), 64.58 (s, 2C), 127.44 (d), 127.57 (d), 129.99 (d), 130.06 (d), 131.13 (s), 136.61 (s, 2C), 136.70 (s, 2C), 137.35 (d), 137.49 (d), 138.70 (s, 2C), 139.49 (s, 2C), 140.61 (s, 2C), 141.31 (s, 2C), 141.50 (s, 2C), 142.07 (s, 2C), 142.12 (s, 2C), 142.37 (s, 2C), 143.39 (s, 2C), 143.81 (s, 2C), 144.39 (s, 2C), 145.45 (s, 2C), 145.78 (s, 2C), 145.86 (s, 2C), 145.89 (s, 2C), 146.04 (s, 2C), 146.08 (s, 2C), 146.35 (s, 2C), 146.76 (s, 2C), 146.88 (s, 2C), 146.97 (s, 2C), 147.676 (s, 2C), 148.57 (s, 2C), 150.09 (s, 2C), 152.80 (s, 2C), 161.93 (s, 2C), 163.77 (s, 2C); ^{29}Si-NMR (80 MHz, 1:1 $CDCl_3$–CS_2) δ −3.99; FAB MS 1199–1202 ($M^+ + 1$ cluster).

4c: ^{1}H-NMR (500 MHz, 1:3 $CDCl_3$–CS_2) δ 1.47 (s, 9H), 4.85 (s, 1H), 7.4–7.6 (m, 6H), 8.07 (d, 2H, $J = 7.7$ Hz), 8.22 (d, 2H, $J = 7.7$ Hz); ^{13}C-NMR (126 MHz, 1:3 $CDCl_3$–CS_2) 621.53 (s), 29.18 (q), 48.84 (d, 1C), 60.69 (s, 1C), 127.68 (d, two carbons), 130.12(d), 130.16 (d), 130.48(q), 130.87 (q), 136.48 (s, 1C), 137.71 (d), 137.85 (d), 138.09 (s, 1C), 138.19 (s, 1C), 138.37 (s, 1C), 139.65(s, 1C), 140.81(s, 1C), 141.49 (s, 1C), 141.58 (s, 1C), 141.76 (s, 1C), 141.80 (s, 1C), 142.14 (s, 1C), 142.25 (s, 1C), 142.40(s, 1C), 142.60(s, 1C), 142.72 (s, 1C), 142.88(s, 1C), 142.93 (s, 1C), 142.97 (s, 1C), 142.99 (s, 1C), 143.08 (s, 1C), 143.67 (s, 1C), 143.87 (s, 2C),

Table 5
Selected bond angles (°)

Si(2)–Si(1)–Si(3)	107.59(9)	C(76)–Si(8)–C(78)	109.4(5)	C(13)–C(14)–C(15)	121.2(5)
Si(2)–Si(1)–Si(4)	109.90(8)	C(77)–Si(8)–C(78)	109.1(4)	C(14)–C(15)–C(16)	120.0(5)
Si(2)–Si(1)–C(29)	109.8(1)	Si(5)–C(1)–C(2)	114.7(3)	C(14)–C(15)–C(32)	118.3(4)
Si(3)–Si(1)–Si(4)	111.18(8)	Si(5)–C(1)–C(6)	109.7(3)	C(16)–C(15)–C(32)	108.0(4)
Si(3)–Si(1)–C(29)	109.7(2)	Si(5)–C(1)–C(9)	110.6(3)	C(15)–C(16)–C(17)	118.7(5)
Si(4)–Si(1)–C(29)	108.7(2)	C(2)–C(1)–C(6)	110.1(4)	C(15)–C(16)–C(34)	108.9(5)
Si(1)–Si(2)–C(61)	113.0(3)	C(2)–C(1)–C(9)	110.2(4)	C(17)–C(16)–C(34)	119.4(5)
Si(1)–Si(2)–C(62)	110.5(3)	C(6)–C(1)–C(9)	100.8(4)	C(4)–C(17)–C(16)	121.0(4)
Si(1)–Si(2)–C(63)	108.4(3)	C(1)–C(2)–C(3)	122.2(4)	C(4)–C(17)–C(18)	107.5(5)
C(61)–Si(2)–C(62)	107.9(4)	C(1)–C(2)–C(12)	123.2(4)	C(16)–C(17)–C(18)	119.3(5)
C(61)–Si(2)–C(63)	106.7(4)	C(3)–C(2)–C(12)	107.8(4)	C(17)–C(18)–C(19)	108.3(4)
C(62)–Si(2)–C(63)	110.3(4)	C(2)–C(3)–C(4)	121.4(5)	C(17)–C(18)–C(36)	121.0(5)
Si(1)–Si(3)–C(64)	110.9(3)	C(2)–C(3)–C(14)	108.4(4)	C(19)–C(18)–C(36)	119.6(5)
Si(1)–Si(3)–C(65)	113.4(3)	C(4)–C(3)–C(14)	119.1(4)	C(5)–C(19)–C(18)	108.4(5)
Si(1)–Si(3)–C(66)	108.3(3)	C(3)–C(4)–C(5)	119.5(4)	C(5)–C(19)–C(20)	119.8(4)
C(64)–Si(3)–C(65)	108.0(3)	C(3)–C(4)–C(17)	120.4(5)	C(18)–C(19)–C(20)	120.1(5)
C(64)–Si(3)–C(66)	109.0(4)	C(5)–C(4)–C(17)	108.5(4)	C(19)–C(20)–C(21)	119.8(4)
C(65)–Si(3)–C(66)	107.2(4)	C(4)–C(s)–C(6)	120.1(4)	C(19)–C(20)–C(38)	120.2(5)
Si(1)–Si(4)–C(67)	112.9(2)	C(4)–C(5)–C(19)	107.3(4)	C(21)–C(20)–C(38)	107.8(4)
Si(1)–Si(4)–C(68)	111.1(3)	C(6)–C(5)–C(19)	120.8(4)	C(7)–C(21)–C(20)	119.3(4)
Si(1)–Si(4)–C(69)	108.8(3)	C(1)–C(6)–C(5)	123.7(5)	C(7)–C(21)–C(22)	119.2(4)
C(67)–Si(4)–C(68)	107.4(4)	C(1)–C(6)–C(7)	109.9(4)	C(20)–C(21)–C(22)	108.8(4)
C(67)–Si(4)–C(69)	107.4(4)	C(5)–C(6)–C(7)	119.5(4)	C(21)–C(22)–C(23)	120.6(4)
C(68)–Si(4)–C(69)	109.2(5)	C(6)–C(7)–C(8)	109.1(4)	C(21)–C(22)–C(50)	106.7(4)
Si(6)–Si(5)–Si(7)	110.0(1)	C(6)–C(7)–C(21)	120.8(4)	C(23)–C(22)–C(50)	120.9(5)
Si(6)–Si(5)–Si(8)	109.90(9)	C(8)–C(7)–C(21)	119.9(4)	C(22)–C(23)–C(24)	120.2(4)
Si(6)–Si(5)–C(1)	110.2(2)	C(7)–C(8)–C(9)	108.0(4)	C(22)–C(23)–C(51)	120.4(5)
Si(7)–Si(5)–Si(8)	109.59(9)	C(7)–C(8)–C(24)	120.8(4)	C(24)–C(23)–C(51)	107.1(4)
Si(7)–Si(5)–C(1)	109.7(1)	C(9)–C(8)–C(24)	120.4(5)	C(8)–C(24)–C(23)	119.3(4)
Si(8)–Si(5)–C(1)	107.4(2)	C(1)–C(9)–C(8)	109.8(4)	C(8)–C(24)–C(25)	120.1(4)
Si(5)–Si(6)–C(70)	113.5(3)	C(1)–C(9)–C(10)	124.0(5)	C(23)–C(24)–C(25)	108.5(4)
Si(5)–Si(6)–C(71)	108.7(3)	C(8)–C(9)–C(10)	118.9(4)	C(24)–C(25)–C(26)	119.1(4)
Si(5)–Si(6)–C(72)	112.7(3)	C(9)–C(10)–C(11)	120.6(4)	C(24)–C(25)–C(39)	107.8(4)
C(70)–Si(6)–C(71)	106.3(4)	C(9)–C(10)–C(26)	121.3(4)	C(26)–C(25)–C(39)	120.7(5)
C(70)–Si(6)–C(72)	107.0(4)	C(11)–C(10)–C(26)	107.2(4)	C(10)–C(26)–C(25)	120.1(5)
C(71)–Si(6)–C(72)	108.4(4)	C(10)–C(11)–C(12)	117.2(4)	C(10)–C(26)–C(27)	107.2(4)
Si(5)–Si(7)–C(73)	112.9(4)	C(10)–C(11)–C(28)	108.9(4)	C(25)–C(26)–C(27)	120.2(4)
Si(5)–Si(7)–C(74)	111.0(3)	C(12)–C(11)–C(28)	122.0(4)	C(26)–C(27)–C(28)	108.5(4)
Si(5)–Si(7)–C(75)	108.7(3)	C(2)–C(12)–C(11)	121.9(5)	C(26)–C(27)–C(41)	119.3(4)
C(73)–Si(7)–C(74)	108.1(5)	C(2)–C(12)–C(13)	109.1(4)	C(28)–C(27)–C(41)	122.0(5)
C(73)–Si(7)–C(75)	107.8(5)	C(11)–C(12)–C(13)	117.3(4)	C(11)–C(28)–C(27)	108.1(4)
C(74)–Si(7)–C(75)	108.2(5)	C(12)–C(13)–C(14)	107.5(4)	C(11)–C(28)–C(29)	123.3(4)
Si(5)–Si(8)–C(76)	110.6(3)	C(12)–C(13)–C(30)	120.4(4)	C(27)–C(28)–C(29)	121.6(4)
Si(5)–Si(8)–C(77)	108.8(4)	C(14)–C(13)–C(30)	120.9(4)	Si(1)–C(29)–C(28)	113.5(3)
Si(5)–Si(8)–C(78)	111.5(3)	C(3)–C(14)–C(13)	107.1(4)	Si(1)–C(29)–C(30)	112.2(3)
C(76)–Si(8)–C(77)	107.4(4)	C(3)–C(14)–C(15)	120.8(4)	Si(1)–C(29)–C(43)	110.0(3)
C(28)–C(29)–C(30)	109.7(4)	C(40)–C(39)–C(51)	119.8(4)	C(22)–C(50)–C(58)	118.8(4)
C(28)–C(29)–C(43)	110.1(4)	C(39)–C(40)–C(41)	120.4(4)	C(38)–C(50)–C(58)	120.7(5)
C(30)–C(29)–C(43)	100.5(3)	C(39)–C(40)–C(52)	120.1(5)	C(23)–C(51)–C(39)	107.9(4)
C(13)–C(30)–C(29)	124.3(4)	C(41)–C(40)–C(52)	107.4(5)	C(23)–C(51)–C(59)	118.1(5)
C(13)–C(30)–C(31)	118.0(4)	C(27)–C(41)–C(40)	120.6(5)	C(39)–C(51)–C(59)	120.2(5)
C(29)–C(30)–C(31)	111.0(4)	C(27)–C(41)–C(42)	118.7(4)	C(40)–C(52)–C(53)	109.2(4)
C(30)–C(31)–C(32)	122.0(5)	C(40)–C(41)–C(42)	108.1(4)	C(40)–C(52)–C(60)	119.8(5)
C(30)–C(31)–C(44)	107.3(4)	C(41)–C(42)–C(43)	120.6(4)	C(53)–C(52)–C(60)	120.5(4)
C(32)–C(31)–C(44)	120.7(4)	C(41)–C(42)–C(53)	107.8(4)	C(42)–C(53)–C(52)	107.5(4)
C(15)–C(32)–C(31)	119.6(4)	C(43)–C(42)–C(53)	119 4(4)	C(42)–C(53)–C(54)	121.2(4)
C(15)–C(32)–C(33)	107.7(4)	C(29)–C(43)–C(42)	123.8(4)	C(52)–C(53)–C(54)	119.4(4)
C(31)–C(32)–C(33)	119.5(4)	C(29)–C(43)–C(44)	109.6(4)	C(45)–C(54)–C(53)	119.2(4)
C(32)–C(33)–C(34)	107.7(4)	C(42)–C(43)–C(44)	120.0(4)	C(45)–C(54)–C(55)	107.4(4)
C(32)–C(33)–C(46)	119.6(4)	C(31)–C(44)–C(43)	108.9(4)	C(53)–C(54)–C(55)	120.8(5)
C(34)–C(33)–C(46)	121.2(5)	C(31)–C(44)–C(45)	119.6(4)	C(47)–C(55)–C(54)	108.6(4)
C(16)–C(34)–C(33)	107.8(4)	C(43)–C(44)–C(45)	1205(4)	C(47)–C(55)–C(56)	119.6(5)
C(16)–C(34)–C(35)	121.2(5)	C(44)–C(45)–C(46)	119.7(4)	C(54)–C(55)–C(56)	119.5(5)
C(33)–C(34)–C(35)	119.6(5)	C(44)–C(45)–C(54)	119 7(4)	C(55)–C(56)–C(57)	119.8(5)

Table 5 (*Continued*)

C(34)–C(35)–C(36)	119 9(5)	C(46)–C(45)–C(54)	109.2(4)	C(55)–C(56)–C(60)	120.0(5)
C(34)–C(35)–C(48)	119 4(5)	C(33)–C(46)–C(45)	120.9(4)	C(57)–C(56)–C(60)	108.0(5)
C(36)–C(35)–C(48)	108.0(5)	C(33)–C(46)–C(47)	119.2(5)	C(49)–C(57)–C(56)	120.5(5)
C(18)–C(36)–C(35)	119.3(5)	C(45)–C(46)–C(47)	107.4(4)	C(49)–C(57)–C(58)	119.9(5)
C(18)–C(36)–C(37)	120.4(5)	C(46)–C(47)–C(48)	119.6(5)	C(56)–C(57)–C(58)	107.6(4)
C(35)–C(36)–C(37)	108.2(5)	C(46)–C(47)–C(55)	107.3(4)	C(50)–C(58)–C(57)	119.6(5)
C(36)–C(37)–C(38)	119.9(5)	C(48)–C(47)–C(55)	120 ~ 7(5)	C(50)–C(58)–C(59)	120.3(5)
C(36)–C(37)–C(49)	108.1(5)	C(35)–C(48)–C(47)	121.0(5)	C(57)–C(58)–C(59)	108.9(5)
C(38)–C(37)–C(49)	119.6(5)	C(35)–C(48)–C(49)	107.9(5)	C(51)–C(59)–C(58)	121.5(5)
C(20)–C(38)–C(37)	119.7(5)	C(47)–C(48)–C(49)	119.7(5)	C(51)–C(59)–C(60)	120.0(5)
C(20)–C(38)–C(50)	107.9(4)	C(37)–C(49)–C(48)	107.8(5)	C(58)–C(59)–C(60)	107.6(5)
C(37)–C(38)–C(50)	119.7(5)	C(37)–C(49)–C(57)	120.3(5)	C(52)–C(60)–C(56)	119.8(5)
C(25)–C(39)–C(40)	118.8(5)	C(48)–C(49)–C(57)	119 6(5)	C(52)–C(60)–C(59)	120.0(4)
C(25)–C(39)–C(51)	108.6(5)	C(22)–C(50)–C(38)	108.8(4)	C(56)–C(60)–C(59)	107.9(5)

143.99 (s, 1C), 144.07 (s, 1C), 144.16 (s, 1C), 144.22 (s, 2C), 144.23 (s, 1C), 144.33 (s, 1C), 144.39 (s, 1C), 144.45 (s, 1C), 144.47 (s, 1C), 144.56 (s, 1C), 144.66 (s, 1C), 144.88 (s, 1C), 145.06(s, 1C), 145.13 (s, 1C), 145.30(s, 2C), 145.31 (s, 1C), 146.09(s, 1C), 146.43 (s, 1C), 146.49 (s, 1C), 146.82 (s, 1C), 146.86 (s, 1C), 147.01 (s, 1C), 147.37 (s, 1C), 147.56 (s, 1C), 148.08 (s, 1C), 148.35 (s, 1C), 148.41 (s, 1C), 148.67 (s, 1C), 149.64 (s, 1C), 149.94 (s, 1C), 150.59 (s, 1C), 157.24 (s, 1C), 160.80 (s, 1C); FAB MS 960963 ($M^+ + 1$ cluster); UV–vis (toluene) λ_{max} (nm): 439 (br).

5c: brown solid; ^{1}H-NMR (500 MHz, 1:3 $CDCl_3$–CS_2) δ 1.44 (s, 9H), 7.5–7.7 (m, 6H), 8.05 (d, 2H, $J = 6.8$ Hz), 8.21 (d, 2H, $J = 6.8$ Hz); ^{13}C-NMR (126 MHz, 1:3 $CDCl_3$–CS_2) 522.00 (s), 29.33 (q), 61.32 (s, 1C), 75.82 (s, 1C), 127.95 (d), 127.99 (d), 130.21 (s), 130.50 (s), 130.75 (d), 130.80 (d), 136.95 (s, 1C), 137.20 (s, 1C), 137.44 (s, 1C), 137.85 (d), 137.97 (d), 138.33 (s, 1C), 140.49 (s, 1C), 140.64 (s, 1C), 140.78 (s, 1C), 141.92 (s, 1C), 142.00 (s, 1C), 142.21 (s, 1C), 142.27 (s, 1C), 142.31 (s, 1C), 142.41 (s, 1C), 142.48 (s, 1C), 142.49 (s, 1C), 142.66 (s, 1C), 142.72 (s, 1C), 142.79 (s, 1C), 142.83 (s, 1C), 142.89 (s, 1C), 143.01 (s, 1C), 143.03 (s, 1C), 143.19 (s, 1C), 143.25 (s, 1C), 143.31 (s, 1C), 143.61 (s, 1C), 143.67 (s, 1C), 143.95 (s, 1C), 144.02 (s, 1C), 144.09 (s, 1C), 144.21 (s, 1C), 144.23 (s, 1C), 144.29 (s, 1C), 144.33 (s, 1C), 144.48 (s, 1C), 144.64 (s, 1C), 144.86 (s, 1C), 144.99 (s, 1C), 145.23 (s, 1C), 145.33 (s, 1C), 145.36 (s, 1C), 145.51 (s, 1C), 146.18 (s, 1C), 146.50 (s, 1C), 146.52(s, 1C), 146.59 (s, 1C), 146.70 (s, 1C), 146.92 (s, 1C), 147.22 (s, 1C), 147.62 (s, 1C), 148.02 (s, 1C), 148.14 (s, 1C), 148.41 (s, 1C), 148.47 (s, 1C), 152.55 (s, 1C), 153.36 (s, 1C), 153.62 (s, 1C), 156.56 (s, 1C); MALDI-TOF-MS: 1919 (M^+); UV–vis (toluene) λ_{max} (nm): 450 (br).

3d: dark red needles; ^{1}H-NMR (500 MHz, 1:2 $CDCl_3$–CS_2) 50.38 (s, 54H); ^{13}C-NMR (125 MHz, 1:1 $CDCl_3$–CS_2) δ 2.63 (q), 60.88 (s, 2C), 135.02 (s, 2C), 135.76 (s, 2C), 139.36 (s, 2C), 140.06 (s, 2C), 140.62 (s, 2C), 140.82 (s, 2C), 141.83 (s, 2C), 142.49 (s, 2C), 142.71 (s, 2C), 143.30 (s, 2C), 143.66 (s, 2C), 143.81 (s, 2C), 144.37 (s, 2C), 145.20 (s, 2C), 145.66 (s, 2C), 146.00 (s, 2C), 146.14 (s, 2C), 146.22 (s, 2C), 146.25 (s, 2C), 146.38 (s, 4C), 147.09 (s, 2C), 147.43 (s, 2C), 147.90 (s, 2C), 148.75 (s, 2C), 151.55 (s, 2C), 151.67 (s, 2C), 164.76 (s, 2C), 165.71 (s, 2C); ^{29}Si-NMR (60 MHz, 1:1, $CDCl_3$–CS_2) δ 52.72, -9.95; FAB MS 1215–1218 ($M^+ + 1$ cluster); UV–vis (toluene) λ_{max} (nm): 547, 566.

3e: dark red solid; ^{1}H-NMR(500 MHz, 1:2 $CDCl_3$–CS_2) $\delta = 1.56$ (s, 9H), 1.57 (s, 9H), 7.2–7.4 (m, 3H), 8.0–8.1 (m, 2H); ^{13}C-NMR (125 MHz, 1:1 $CDCl_3$–CS_2) 625.22 (s, 2C), 31.85 (q), 31.89 (q), 65.74 (s, 2C), 127.30 (d), 129.55 (d), 131.66 (s, 1C), 136.40 (s, 2C), 137.11 (d), 138.65 (s, 2C), 139.48 (s, 2C), 140.57 (s, 2C), 141.13 (s, 2C), 141.54 (s, 2C), 141.89 (s, 2C), 141.98 (s, 2C), 142.20 (s, 2C), 143.51 (s, 2C), 143.98 (s, 2C), 144.19(s, 2C), 145.31 (s, 2C), 145.33 (s, 2C), 145.99 (s, 2C), 146.02(s, 2C), 146.11 (s, 2C), 146.14 (s, 2C), 146.36 (s, 2C), 146.59 (s, 2C), 146.94 (s, 2C), 147.39 (s, 2C), 147.72 (s, 2C), 148.57 (s, 2C), 150.31 (s, 2C), 152.74 (s, 2C), 162.66 (s, 2C), 165.19 (s, 2C); ^{29}Si-NMR (60 MHz, 1:1 $CDCl_3$–CS_2) δ 5.22; FAB MS 1159–1162 ($M^+ + 1$ cluster); UV–vis (toluene) λ_{max} (nm): 535.

2f: (we obtained **2f** as a mixture of **2f** and **4f**) ^{1}H-NMR (500 MHz, 1:1 $CDCl_3$–CS_2) 1.73 (s, 9H), 2.39 (s, 3H), 6.97 (s, 1H), 7.29 (d, 2H, $J = 7.8$ Hz), 8.34 (d, 2H, $J = 7.8$ Hz); ^{13}C-NMR (126 MHz, 1:1 $CDCl_3$–CS_2) 621.91 (q), 25.19 (s), 32.31 (q), 60.79 (d, lC),63.34(s, 1C), 129.10(d), 129.26(s), 137.35(d); ^{29}Si-NMR (60MHz, 1:1 $CDCl_3$–CS_2) 57.93.

3f: brown solid; ^{1}H-NMR (500 MHz, 1:1 $CDCl_3$–CS_2) δ 1.54 (s, 9H), 1.56 (s, 9H), 2.31 (s, 3H), 7.09 (d, 2H, $J = 8.0$ Hz), 7.94 (d, 2H, $J = 8.0$ Hz); ^{13}C-NMR (125 MHz, 1:1 $CDCl_3$–CS_2) δ 21.44 (q), 25.22 (s), 31.80 (q), 31.88 (q), 65.96 (s, 2C), 127.90 (s), 128.16 (d), 136.39 (s, 2C), 137.18 (d), 137.18 (s, 2C), 138.65 (s, 2C), 139.27 (s), 139.54 (s, 2C), 140.55(s, 2C), 141.15(s, 2C), 141.54 (s, 2C), 141.90 (s, 2C), 141.99 (s, 2C), 142.22 (s, 2C), 143.50 (s, 2C), 143.99 (s, 2C), 144.16 (s, 2C), 145.32 (s, 2C), 145.38 (s, 2C), 145.99 (s, 2C), 146.05 (s, 2C), 146.10(s, 2C), 146.15 (s, 2C), 146.40 (s, 2C), 146.63 (s, 2C), 146.97 (s, 2C), 147.42 (s, 2C), 147.72 (s, 2C), 148.58 (s, 2C), 150.38 (s, 2C), 152.82 (s, 2C), 162.92 (s, 2C), 165.37 (s, 2C); 29Si-NMR (60 MHz, 1:1 $CDCl_3$–CS_2) δ 5.55; FAB MS 1186–1189 ($M^+ + 1$ cluster); UV–vis (toluene) λ_{max} (nm): 533 (br).

4f: brown solid; ^{1}H-NMR(500 MHz, 1:1 $CDCl_3$–CS_2)51.51 (s, 9H), 1.70 (s,9H), 2.51 (s, 3H), 5.44 (s, 1H), 7.37 (d, 2H, $J = 7.9$ Hz), 7.23 (d, 2H, $J = 7.9$ Hz); ^{13}C-NMR (126 MHz, 1:1 $CDCl_3$–CS_2) δ 21.61 (q), 24.70 (s), 24.71 (s), 32.24 (q), 32.34 (q), 49.54 (d, 1C), 62.37 (s, 1C), 128.43 (d), 128.91 (s), 136.39 (s, 1C), 137.55 (d), 138.23 (s, 1C), 138.41 (s, 1C), 138.66 (s, 1C), 139.92 (s), 140.85 (s, 1C), 141.82 (s, 2C), 141.86 (s, 1C), 142.02 (s, 1C), 142.16 (s, 1C), 142.36 (s, 1C), 142.38 (s, 1C), 142.72 (s, 1C), 142.90 (s, 1C), 143.04 (s, 1C), 143.06 (s, 1C), 143.14 (s, 1C), 143.16 (s, 1C), 143.18 (s, 1C), 143.25 (s, 1C), 143.50 (s, 1C), 143.76 (s, 2C), 143.89 (s, 1C), 144.17 (s, 1C), 144.34 (s, 2C), 144.38 (s, 1C), 144.45 (s, 1C), 144.55 (s, 2C), 144.60 (s, IC), 144.89 (s, 2C), 145.04 (s, 1C), 145.13 (s, 1C), 145.22 (s, 1C), 145.33 (s, 1C), 145.53 (s, 2C), 146.28 (s, 2C), 146.65 (s, 1C), 146.92 (s, 1C), 146.97 (s, 1C), 147.03 (s, 1C), 147.18 (s, 1C), 147.48 (s, 1C), 147.69 (s, 1C), 148.29 (s, 1C), 148.48 (s, 1C), 148.80 (s, 1C), 148.93 (s, 1C), 150.06 (s, 1C), 150.08 (s, 1C), 151.82 (s, 1C), 157.16 (s, 1C), 161.84 (s, 1C);^{29}Si-NMR(60 MHz, 1:1 $CDCl_3$–CS_2) 33.59; FAB MS 954–957($M^+ + 1$ cluster); UV–vis (toluene) λ_{max} (nm): 436 (br).

5f: brown solid; ^{1}H-NMR (500 MHz, 1:1 $CDCl_3$–CS_2) δ 1.41 (s, 9H), 1.69 (s, 9H), 2.55 (s, 3H), 7.49 (d, 2H, $J = 7.9$ Hz), 8.17 (d, 2H, $J = 7.9$ Hz); ^{13}C-NMR (126 MHz, 1:1 $CDCl_3$–CS_2) 621.48 (q), 24.57 (s), 24.86 (s), 31.97 (q), 32.12 (q), 62.19 (s, 1C), 75.49 (s, 1C), 127.68 (s), 128.89 (d), 136.93 (s, 1C), 137.22 (s, 1C), 137.61 (s, 1C), 137.61 (d), 138.93 (s, 1C), 140.56 (s, 1C), 140.62 (s, 1C), 140.79 (s, 1C), 141.06 (s), 141.91 (s, 1C), 141.97 (s, 1C), 142.07 (s, 2C), 142.14 (s, 1C), 142.17 (s, 1C), 142.32 (s, 1C), 142.35 (s, 1C), 142.48 (s, 2C), 142.75 (s, 1C), 142.79 (s, 1C), 142.93 (s, 1C), 142.99 (s, 1C), 143.10 (s, 1C), 143.17 (s, 1C), 143.32 (s, 1C), 143.40 (s, 1C), 143.45 (s, 1C), 143.48 (s, 1C), 143.67(s, 1C), 143.73(s, 1C), 144.06 (s, 1C), 144.09 (s, 1C), 144.14 (s, 1C), 144.26 (s, 1C), 144.36 (s, 1C), 144.45 (s, 1C), 144.62 (s, 1C), 144.87 (s, 1C), 145.26 (s, 1C), 145.31 (s, 1C), 145.37 (s, 1C), 145.50 (s, 1C), 145.65 (s, 1C), 146.09 (s, 1C), 146.36 (s, 1C), 146.41 (s, 1C), 146.49 (s, 1C), 146.64 (s, 1C), 146.74 (s, 1C), 146.84 (s, 1C), 147.58 (s, 1C), 147.74(s, 1C), 148.28 (s, 2C), 148.60(s, 1C), 152.88 (s, 1C), 153.26 (s, 1C), 154.24 (s, 1C), 156.83 (s, 1C); ^{29}Si-NMR (80 MHz, 1:1 $CDCl_3$–CS_2) δ 6.17; MALDI-TOF-MS: 1907 (M^+).

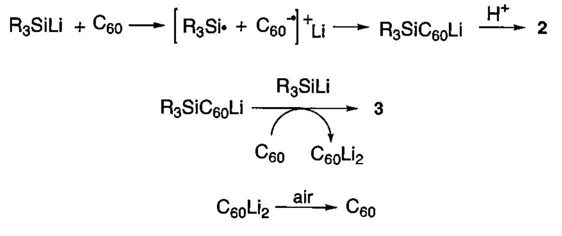

Scheme 2.

3g: brown solid; ^{1}H-NMR (500 MHz, 1:1 $CDCl_3$–CS_2) δ 1.43 (s, 9H), 2.35 (s, 3H), 2.36 (s, 3H), 7.12 (d, 2H, $J = 7.7$ Hz), 7.17 (d, 2H, $J = 7.7$ Hz), 7.83 (d, 2H, $J = 7.7$ Hz), 7.89 (d, 2H, $J = 7.7$ Hz); ^{13}C-NMR (126 MHz, 1:1 $CDCl_3$–CS_2) d 21.61 (q), 21.63 (q), 22.32 (s), 29.12 (q), 64.99 (s, 2C), 127.61 (s), 127.67 (s), 128.26 (d), 128.35 (d), 136.52 (s, 2C), 136.74 (s, 2C), 137.40 (d), 137.51 (d), 138.68 (s, 2C), 139.59 (s, 2C), 139.72 (s), 139.76 (s), 140.55 (s, 2C), 141.30 (s, 2C), 141.47 (s, 2C), 142.07 (s, 2C), 142.14 (s, 2C), 142.34 (s, 2C), 143.36 (s, 2C), 143.80 (s, 2C), 144.29 (s, 2C), 145.44 (s, 2C), 145.86 (s, 2C), 145.88 (s, 4C), 146.01 (s, 2C), 146.06 (s, 2C), 146.40 (s, 2C), 146.81 (s, 2C), 146.93 (s, 2C), 147.00 (s, 2C), 147.74 (s, 2C), 148.55 (s, 2C), 150.22 (s, 2C), 152.90 (s, 2C), 162.39 (s, 2C), 164.07 (s, 2C); 29Si-NMR (80 MHz, 1:1 CDCI3CS2) 6–3.71; FAB MA 1255–1257 ($M^+ + 1$ cluster).

4g: brown solid; ^{1}H-NMR (500 MHz, 1:1 $CDCl_3$–CS_2) δ 1.44 (s, 9H), 2.47 (s, 6H), 7 31 (d, 2H, $J = 7.9$ Hz), 7.33 (d, 2H, $J = 7.9$ Hz), 7.95 (d, 2H, $J = 7.9$ Hz), 8.09 (d, 2H, $J = 7.9$ Hz); ^{13}C-NMR (126 MHz, 1:1 $CDCl_3$–CS_2) 621.71 (q, two carbon), 22.74 (s), 29.31 (q), 49.06 (d, 1C), 61.27 (s, 1C), 127.03 (s), 127.45 (s), 128.55 (d), 136.42 (s, 1C), 137.93 (d), 138.05 (d), 138.09 (s, 1C), 138.16 (s, 1C), 138.33 (s, 1C), 138.49 (s), 139.90 (s, 1C), 140.12 (s), 140.15 (s), 140.85 (s, 1C), 141.62 (s, 1C), 141.66 (s, 1C), 141.92 (s, 1C), 141.95 (s, 1C), 142.24 (s, 1C), 142.34 (s, 1C), 142.51 (s, 1C), 142.70 (s, 2C), 142.84 (s, 1C), 142.94 (s, 1C), 142.98 (s, 2C), 143.07 (s, 1C), 143.08 (s, 1C), 143.13 (s, 1C), 143.21(s, 1C), 143.73 (s, 1C), 144.05 (s, 1C), 144.07(s, 1C), 144.21 (s, 1C), 144.30 (s, 1C), 144.33 (s, 1C), 144.37 (s, 1C), 144.39 (s, 1C), 144.46 (s, 1C), 144.55 (s, 2C), 144.82(s, 2C), 144.99(s, 1C), 145.16(s, 1C), 145.30(s, 1C), 145.41 (s, 1C), 145.51 (s, 1C), 146.33 (s, 1C), 146.62 (s, 1C), 146.64 (s, 1C), 146.98 (s, 2C), 147.13 (s, 1C), 147.49 (s, 1C), 147.68 (s, 1C), 148.19 (s, 1C), 148.48 (s, 1C), 148.65 (s, 1C), 148.95 (s, 1C), 149.90 (s, 1C), 153.18 (s, 1C), 151.01 (s, 1C), 157.59 (s, 1C), 161.31 (s, 1C); ^{29}Si-NMR (80 MHz, 1:1 $CDCl_3$–CS_2) δ -3.56; FAB MS 989–991 ($M^+ + 1$ cluster); UV–vis (toluene) λ_{max} (nm): 440 (br).

5g: brown solid; ^{1}H-NMR (500 MHz, 1:1 $CDCl_3$–CS_2) δ 1.37 (s, 9H), 2.45 (s, 3H), 2.47 (s, 3H), 7.35 (d, 2H, $J = 7.8$ Hz), 7.38 (d, 2H, $J = 7.8$ Hz), 7.90 (d, 2H, $J = 7.8$ Hz), 8.08 (d, 2H, $J = 7.8$ Hz); ^{13}C-NMR (126 MHz, 1:1 $CDCl_3$–CS_2) d 21.59 (q), 21.63 (q), 22.17 (s), 29.45 (q), 61.93 (s, 1C), 75.94 (s, 1C), 126.69 (s), 127.03

(s), 128.87 (d), 128.89 (d), 137.30 (s, 1C), 137.42 (s, 1C), 138.05 (d), 138.20 (d), 138.47 (s, 1C), 140.55 (s, 1C), 140.73 (s, 1C), 141.00 (s), 141.05 (s, 1C), 141.09 (s), 142.05 (s, 1C), 142.15 (s, 1C), 142.32 (s, 1C), 142.40 (s, 2C), 142.51 (s, 2C), 142.55 (s, 1C), 142.80 (s, 1C), 142.86 (s, 1C), 142.93 (s, 1C), 142.95 (s, 2C), 143.01 (s, 1C), 143.10 (s, 1C), 143.15 (s, 1C), 143.31 (s, 1C), 143.36 (s, 1C), 143.44 (s, 1C), 143.76 (s, 1C), 143.81 (s, 1C), 144.11 (s, 1C), 144.15 (s, 1C), 144.27 (s, 1C), 144.30 (s, 1C), 144.35 (s, 1C), 144.39 (s, 1C), 144.55 (s, 1C), 144.61 (s, 1C), 144.79 (s, 1C), 145.05 (s, 1C), 145.09 (s, 1C), 145.36 (s, 1C), 145.46 (s, 1C), 145.55 (s, 1C), 145.66 (s, 1C), 146.28 (s, 1C), 146.62(s, 1C), 146.63 (s, 1C), 146.71 (s, 1C), 146.84 (s, 1C), 147.03 (s, 1C), 147.26 (s, 1C), 147.71 (s, 1C), 148.20 (s, 1C), 148.39 (s, 1C), 148.54 (s, 1C), 148.65 (s, 1C), 153.02 (s, 1C), 153.36 (s, 1C), 153.96 (s, 1C), 156.95 (s, 1C); ^{29}Si-NMR (80 MHz, 1:1 $CDCl_3$–CS_2) δ -2.61; MALDI-TOF-MS 1975 (M^+).

3h: red brown solid; ^{1}H-NMR (500 MHz, 1:1 $CDCl_3$-CS_2) δ 1.63 (s, 9H), 1.64 (s, 9H), 7.2–7.3 (m, 3H), 7.9–8.0 (m, 2H); ^{13}C-NMR (126 MHz, 1:1 $CDCl_3$–CS_2) δ 31.80 (q), 31.83 (q), 34.33 (s), 68.73 (s, 2C), 127.75 (d), 129.01 (d), 135.50 (s, 2C), 136.39 (s, 2C), 136.43 (d), 137.57 (s, 2C), 138.99 (s, 2C), 140.18 (s, 2C), 140.59 (s, 2C), 141.63 (s, 2C), 142.32 (s, 2C), 142.34 (s, 2C), 142.56 (s, 2C), 143.70 (s, 2C), 143.84 (s, 2C), 144.28 (s, 2C), 145.72 (s, 2C), 145.86 (s, 2C), 146.00 (s, 2C), 146.06 (s, 2C), 146.19 (s, 2C), 145.24 (s, 2C), 147.12 (s, 2C), 147.25 (s, 2C), 147.33 (s, 2C), 147.80 (s, 2C), 148.63 (s, 2C), 150.41 (s, 2C), 152.46 (s, 2C), 164.06 (s, 2C), 164.59 (s, 2C); FAB MS 1245–1253 ($M^+ + 1$ cluster).

2i: brown solid; ^{1}H-NMR (500 MHz, 1:1 $CDCl_3$-CS_2) δ 1.66 (d, 6H, $J = 7.6$ Hz), 2.60 (sept, 2H, $J = 7.5$ Hz), 6.95 (s, 1H), 7.4–7.6 (m, 3H), 8.04 (d, 2H, $J = 7.9$ Hz); ^{13}C-NMR (125 MHz, 1:1 $CDCl_3$–CS_2) δ 17.70 (d), 20.70 (q), 20.96 (q), 59.16 (d, 1C), 62.12 (s, 1C), 133.79 (s, 2C), 134.17 (s), 135.75 (d), 135.86 (s, 2C), 140.09 (s, 2C), 140.56 (s, 2C), 141.38 (s, 2C), 141.46 (s, 2C), 141.52 (s, 2C), 141.64 (s, 2C), 141.81 (s, 2C), 142.43 (s, 2C), 142.51 (s, 2C), 142.68 (s, 2C), 143.57 (s, 2C), 144.26 (s, 2C), 144.54 (s, 2C), 144.80 (s, 2C), 145.30 (s, 2C), 145.55 (s, 2C), 145.56 (s, 2C), 146.04 (s, 2C), 146.22(s, 2C), 146.28(s, 2C), 146.37 (s, 2C), 146.43 (s, 2C), 146.63 (s, 1C), 146.73 (s, 2C), 14?.33 (s, 1C), 147.81 (s, 2C), 154.14 (s, 2C), 158.00 (s, 2C); FAB MS 954–960 ($M^+ + 1$ cluster).

3.8. Crystallographic analysis

Crystals of suitable for X-ray analysis of the following dimensions were prepared by slowly cooling hexane solutions: 0.10 × 0.20 × 0.40 mm for **3d**CS_2. Diffraction measurements were made on Enraf–Nonius CAD4 computer controlled Kappa axis diffractometer by using graphite-monochromatized Cu–K_α radiation. The unit cells were determined and ref ~ ned from 25 randomly selected reflections obtained by using the CAD4 automatic search, center, index and least-squares routines. Crystal data and data collection parameters and the results of the analyses are listed in Table 3. All data processing was performed on a Silicon Graphics INDIGO computer by using the teXsan structure solving program. All intensities were corrected for Lorenz and polarization correction. Neutral atom scattering factors were calculated by the standard procedures. An anomalous dispersion correction was applied to all nonhydrogen atoms. Full-matrix least-squares refinements minimized the function $\Sigma\omega(|F_o| - |^F_c|^2$, $\omega = 1$.

Compound **3d** crystallized in the triclinic crystal system. The $\omega - 2\theta$ scan technique was adopted varying ω scan width as function of θ (ω scan width $= 0.5 + 0.150 \tan\theta$). Removal of redundant data left 9350 unique data in the final data set. The structure was solved by direct method (SIR) and refined via standard least-squares and difference Fourier techniques. Hydrogen atoms were located and added to the structure factor calculations but their positions were not refined.

4. Supporting information available

Detailed information of the X-ray crystal analysis for **3d** and figures giving additional NMR spectra for **2**, **3**, **4**, **5** (63 pages). Ordering information is given on any current masthead page.

Acknowledgements

This work was supported by a Grant-in-Aid for Scientific Research from the Ministry of Education, Science and Culture of Japan.

References

[1] A. Hirsch, Angew. Chem. Int. Ed. Engl. 32 (1993) 1138.

[2] G. Hammond, V.J. Kuck (Eds.), Fullerenes: Synthesis, Propernes, and Chemistry of Large Carbon Clusters, ACS Symposium Series 481, American Chemical Society, Washington DC, 1992.

[3] A. Hirsch, The Chemistry of the Fullerenes, Thime Verlag, Stuttgart, 1994.

[4] (a) F. Wudl, A. Hirsch, K.C. Khemani, T. Suzuki, P.-M. Allemand, A. Koch, H. Eckert, G. Srdanov, H. Webb, In the ref. 4, pp. 161–175. (b) P.J. Fagan, P.J. Krusic, D.H. Evans, S.A. Leake, E. Johnston, J. Am. Chem. Soc. 114 (1992) 9697. (c) A. Hirsch, A. Soi, H.R. Karfunckel, Angew. Chem. Int Ed. Engl. 31, (1992) 766. (d) A. Hirsch, T. Grosser, A. Skiebe, A. Soi, Chem. Ber. 126 (1993) 1061. (e) H. Nagashima, H. Terasaki, E.

Kimura, K. Nakajima, K. Itoh, J. Org. Chem. 59 (1994) 1246. (f) H.L. Anderson, R. Faust, Y. Rubin, F. Diederich, Angew. Chem. Int. Ed. Engl. 33 (1994) 1366. (g) M. Murata, K. Komatsu, T.S. M. Wan, Tetrahedron Lett. 37 (1996) 7061.

[5] Preliminary results were communicated in: T. Kusukawa, W. Ando, Angew. Chem. Int. Ed. Engl. 35 (1996) 1315.

[6] Reactivity of C_{60} dimer with Bu_3SnH: see reference ([4]b).

[7] In the case of 1,4-addition shows a rather broad absorption around 440 nm (see reference ([4]g)).

[8] N. Matsuzawa, D.A. Dixon, T. Fukunaga, J. Phys. Chem. 96 (1992) 7594.

[9] HOMO levels of hydrosilanes (ev) calculated by PM3 and AM1 are as follows: $(Me_3Si)_3SiH$, −8.60, −9.24; *tert*-Bu_2(4-Me-C_6H_4)SiH, −9.01, −9.22; *tert*-Bu(4-MeC_6H_4)$_2$SiH, −9.02, −9.23; *tert*-Bu_2PhSiH, −9.16, −9.45; *tert*-BuPh_2SiH, −9.20, −9.49; *iso*-Pr_2PhSiH, −9.22, −9.50; *iso*-PrPh_2SiH, −9.29, −9.52; Et_2PhSiH, −9.30, −9.53; MePh_2SiH, −9.36, −9.59; Ph_3SiH, −9.36, −9.52; Me_2PhSiH, −9.39, −9.62; EtPh_2SiH, −9.41, −9.59.

[10] J.B. Lambert, M. Urdaneta-Pérez, J. Am. Chem. Soc. 100 (1978) 157.

[11] P. Cuadrao, A.M. González, B. González, F.J. Pulido, Synth. Commun. 19 (1989) 275.

[12] T. Iwahara, R. West, Chem. Lett. (1991) 545.